

## Anthryl-Doped Conjugated Polyelectrolytes as Aggregation-Based Sensors for Nonquenching Multicationic Analytes

Andrew Satrijo and Timothy M. Swager\*

Contribution from the Department of Chemistry, Massachusetts Institute of Technology,  
77 Massachusetts Avenue, Cambridge, Massachusetts 02139

Received July 25, 2007; E-mail: tswager@mit.edu

**Abstract:** The fluorescence-based detection of nonquenching, multicationic small molecules has been demonstrated using a blue-emitting, polyanionic poly(*p*-phenylene ethynylene) (PPE) doped with green-emitting exciton traps (anthryl units). Multicationic amines (spermine, spermidine, and neomycin) were found to effectively induce the formation of tightly associated aggregates between the polymer chains in solution. This analyte-induced aggregation, which was accompanied by enhanced exciton migration in the PPE, ultimately led to a visually noticeable blue-to-green fluorescence color change in the solution. The aggregation-based sensor exhibited poor sensitivity toward dicationic and monocationic amines, demonstrating that a conjugated polyelectrolyte sensor relying on nonspecific, electrostatic interactions may still attain a certain level of selectivity.

### Introduction

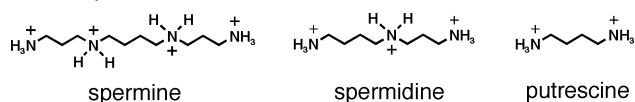
Conjugated polyelectrolytes (CPEs), which are conjugated polymers functionalized with multiple ionic groups, have gained significant interest for chemical and biosensing applications.<sup>1–4</sup> Most CPE sensors rely on a change in the fluorescence intensity of the polymer upon binding of an analyte.<sup>5</sup> Two of the most widely exploited processes for directly quenching the inherent fluorescence intensity of a CPE are electron transfer and energy transfer between the polymer and a quenching species.<sup>6</sup> An analyte that cannot participate in these direct quenching mechanisms (due to incompatible redox and spectral properties, in relation to the photoexcited polymer) is herein described as “nonquenching”.<sup>7,8</sup> However, nonquenching analytes may indirectly cause fluorescence quenching by inducing aggregation of the fluorescent species via electrostatic or hydrophobic interactions, leading to self-quenching processes.<sup>9</sup> Fluorescence self-quenching is any interaction between an excited molecule,

$M^*$ , and a ground-state molecule of the same type,  $M$ , that leads to fluorescence quenching of  $M^*$ .<sup>10</sup>

In addition to promoting self-quenching processes, analyte-induced aggregation can also enhance the exciton transport properties of a conjugated polymer by increasing the number of accessible exciton migration pathways.<sup>11–14</sup> For example, in a dilute, well-dissolved CPE solution, exciton transport can be approximated by a one-dimensional random walk within an isolated polymer chain. However, if the polymers are aggregated within close proximity to each other, interchain exciton migration becomes possible, and a three-dimensional random walk becomes available to the migrating exciton.<sup>11</sup> This enhanced exciton transport in conjugated polymer aggregates increases the probability that an exciton will find a specific site (e.g., a binding site containing a quenching analyte) in the conjugated polymer. This phenomenon of aggregation-enhanced exciton migration can explain the extremely large quenching responses of many CPE-based fluorescent chemical sensors reported in the literature.<sup>3,13–15</sup> In competition with fluorescence quenching mechanisms, energy transfer to emissive low-energy sites may also occur in photoexcited conjugated polymers. Therefore, aggregation-enhanced exciton migration can also lead to en-

- (1) Pinto, M. R.; Schanze, K. S. *Synthesis* **2002**, 1293–1309.
- (2) McQuade, D. T.; Pullen, A. E.; Swager, T. M. *Chem. Rev.* **2000**, *100*, 2537–2574.
- (3) Thomas, S. W.; Joly, G. D.; Swager, T. M. *Chem. Rev.* **2007**, *107*, 1339–1386.
- (4) Ambade, A. V.; Sandanaraj, B. S.; Klaikherd, A.; Thayumanavan, S. *Polym. Int.* **2007**, *56*, 474–481.
- (5) Achyuthan, K. E.; Bergstedt, T. S.; Chen, L.; Jones, R. M.; Kumaraswamy, S.; Kushon, S. A.; Ley, K. D.; Lu, L.; McBranch, D.; Mukundan, H.; Rimsland, F.; Shi, X.; Xia, W.; Whitten, D. G. *J. Mater. Chem.* **2005**, *15*, 2648–2656.
- (6) Liu, M.; Kaur, P.; Waldeck, D. H.; Xue, C. H.; Liu, H. Y. *Langmuir* **2005**, *21*, 1687–1690.
- (7) Lissi, E.; Abiun, E. In *Solubilization in Surfactant Aggregates*; Christian, S. D., Scamehorn, J. F., Eds.; Marcel Dekker: New York, 1995; pp 297–332.
- (8) Lee, J. H.; Carraway, E. R.; Hur, J.; Yim, S.; Schlautman, M. A. *J. Photochem. Photobiol., A* **2007**, *185*, 57–61.
- (9) Kim, J.; McQuade, D. T.; McHugh, S. K.; Swager, T. M. *Angew. Chem., Int. Ed.* **2000**, *39*, 3868–3872.

- (10) Turro, N. J. *Modern Molecular Photochemistry*; University Science Books: Sausalito, CA, 1991.
- (11) Levitsky, I. A.; Kim, J.; Swager, T. M. *J. Am. Chem. Soc.* **1999**, *121*, 1466–1472.
- (12) Hennebicq, E.; Pourtois, G.; Scholes, G. D.; Herz, L. M.; Russell, D. M.; Silva, C.; Setayesh, S.; Grimsdale, A. C.; Müllen, K.; Brédas, J.-L.; Beljonne, D. *J. Am. Chem. Soc.* **2005**, *127*, 4744–4762.
- (13) Tan, C. Y.; Pinto, M. R.; Schanze, K. S. *Chem. Commun.* **2002**, 446–447.
- (14) Jiang, H.; Zhao, X. Y.; Schanze, K. S. *Langmuir* **2006**, *22*, 5541–5543.
- (15) Dwight, S. J.; Gaylord, B. S.; Hong, J. W.; Bazan, G. C. *J. Am. Chem. Soc.* **2004**, *126*, 16850–16859.

**Scheme 1.** Structures of the Fully Protonated Polyamines Used in This Study

hanced fluorescence from emissive low-energy sites, such as defects or dopants, dispersed throughout the conjugated polymer.<sup>16</sup>

Aggregation-enhanced energy transfer to emissive low-energy sites has been recently utilized by Bazan et al. for developing CPE-based DNA sensors.<sup>17,18</sup> Their sensing platform involved the interpolyelectrolyte complexation between the polyanionic macromolecule, DNA, and a polycationic poly(flourene-*alt*-1,4-phenylene) derivative containing a small fraction (1–7%) of 2,1,3-benzothiadiazole (BT) units. When the concentration of DNA increased, the degree of polymer–DNA complexation also increased, which consequentially led to more interchain contacts between the conjugated polymers. The authors proposed that the increased aggregation of the polymer facilitated efficient energy migration from the higher-energy, blue-emitting poly(flourene-*alt*-1,4-phenylene) segments to the lower-energy, green-emitting BT units. As a result, the fluorescence color of the polymer solution changed from blue to green upon the introduction of DNA.

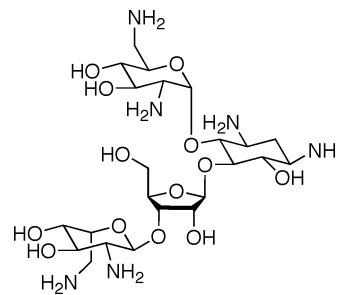
In this study, we investigate aggregation-enhanced exciton migration in a polyanionic poly(*p*-phenylene ethynylene) (PPE) containing green-emitting exciton trap sites. We found that this polymer exhibited a visually noticeable blue-to-green fluorescence color change upon aggregation in poor solvents and in the presence of nonquenching, multicationic, small-molecule analytes. Furthermore, we demonstrate that this fluorescence color-changing sensor could detect biologically relevant, small-molecule analytes, such as spermine, spermidine, and neomycin, at concentration levels suitable for medical<sup>19</sup> and food monitoring<sup>20</sup> applications.

The natural polyamines (e.g., spermine, spermidine, and putrescine) are small aliphatic amines (Scheme 1) that are found in virtually all eukaryotic cells and play a significant role in regulating cell growth and differentiation.<sup>19,21–23</sup> In 1971, Russell reported that polyamines were excreted in abnormally high amounts in the urine of cancer patients; therefore, polyamines were proposed to be possible biochemical markers for malignant tumors.<sup>24</sup> In 1980, Fujita et al. used an electrophoretic analysis to reliably determine the urinary polyamine concentrations for cancer patients and healthy volunteers (Table

**Table 1.** Urinary Spermine and Spermidine Concentrations in Cancer Patients and Healthy Volunteers<sup>a</sup>

	[spermine]		[spermidine]	
	mg/g creatinine	$\mu\text{mol/L}^b$	mg/g creatinine	$\mu\text{mol/L}^b$
normal	$0.18 \pm 0.04$	1.2	$1.32 \pm 0.05$	11.9
solid tumors	$1.23 \pm 0.24$	7.93	$2.90 \pm 0.40$	26.0
blood tumors	$1.47 \pm 0.50$	9.47	$4.77 \pm 0.91$	42.8

<sup>a</sup> Adapted from ref 25. <sup>b</sup> Calculated using a urinary creatinine concentration of 130.4 mg/dL; see ref 27.

**Scheme 2.** Structure of Neomycin

1).<sup>25</sup> In addition to these studies, numerous other investigations have confirmed the higher urinary polyamine concentrations in cancer patients, and it has been proposed that the determination of these concentrations can be used for assessing the effectiveness of cancer chemotherapy and detecting cancer remission and relapse.<sup>26</sup>

Another nonquenching, multicationic, small-molecule analyte of biological importance is neomycin (Scheme 2), which is an aminoglycoside antibiotic used in veterinary medicine. However, neomycin can be ototoxic and nephrotoxic to humans and animals,<sup>28</sup> so its concentration is regulated in livestock products. To protect consumers, the European Union established maximum residue limits for neomycin: 1500 mg/kg for milk, 500 mg/kg for meat, fat, liver, and eggs, and 5000 mg/kg for kidneys.<sup>20</sup>

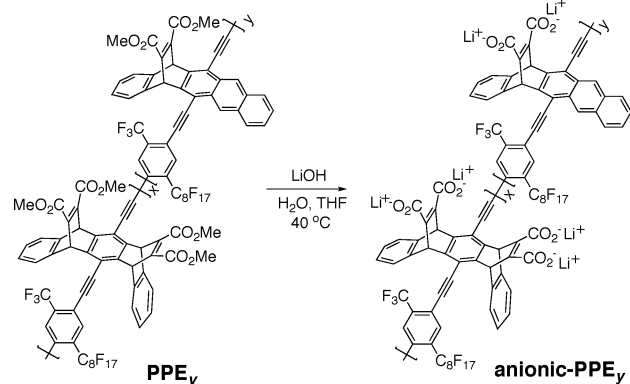
Neomycin, spermine, and spermidine are currently detected using immunoassays, electrophoretic analysis, and chromatographic techniques, which can be relatively slow and require expensive equipment.<sup>23,29</sup> Therefore, the rapid, visual detection of these analytes using a fluorescent CPE sensor may be more suitable for screening a large number of samples and for preliminary analyses.

## Results and Discussion

**Synthesis.** In a previous report, we detailed our investigations on aggregation-enhanced luminescence from emissive, low-energy defect sites in conjugated polymers.<sup>16</sup> During these investigations, we synthesized a series of anthryl-doped poly(*p*-phenylene ethynylene)s, labeled as PPE<sub>y</sub> in Scheme 3, where the subscript *y* denotes the molar percentage of anthryl dopants of the total diacetylene comonomers added into the polymerization reaction. Notably, we showed that even the undoped PPE<sub>0</sub> contained some anthryl defects although in smaller quantities

- (16) Satrijo, A.; Kooi, S. E.; Swager, T. M. *Macromolecules* [Online early access]. DOI: 10.1021/ma071659t. Published online: November 17, 2007.
- (17) Liu, B.; Bazan, G. C. *J. Am. Chem. Soc.* **2004**, *126*, 1942–1943.
- (18) Hong, J. W.; Hemme, W. L.; Keller, G. E.; Rinke, M. T.; Bazan, G. C. *Adv. Mater.* **2006**, *18*, 878–882.
- (19) *Polyamines as Biochemical Markers of Normal and Malignant Growth*; Russell, D. H., Durie, B. G. M., Eds.; Raven Press: New York, 1978.
- (20) Commission Regulation (EC) No 1181/2002 of 1 July 2002 amending Annex I of Council Regulation (EEC) No 2377/90 laying down a Community procedure for the establishment of maximum residue limits of veterinary medicinal products in foodstuffs of animal origin. *Off. J. Eur. Communities: Legis.* **2002**, L172/13–L172/20.
- (21) *Polyamines in Biomedical Research*; Gaugas, J. M., Ed.; Wiley: New York, 1980.
- (22) *Polyamine Protocols*; Morgan, D. M. L., Ed.; Humana Press: Totowa, NJ, 1998.
- (23) Teti, D.; Visalli, M.; McNair, H. *J. Chromatogr., B* **2002**, *781*, 107–149.
- (24) Russell, D. H. *Nat. New Biol.* **1971**, *233*, 144–145.

- (25) Fujita, K.; Nagatsu, T.; Shinpo, K.; Maruta, K.; Teradaira, R.; Nakamura, M. *Clin. Chem.* **1980**, *26*, 1577–1582.
- (26) For a recent review, see: Bachrach, U. *Amino Acids* **2004**, *26*, 307–309.
- (27) Barr, D. B.; Wilder, L. C.; Caudill, S. P.; Gonzalez, A. J.; Needham, L. L.; Pirkle, J. L. *Environ. Health Perspect.* **2005**, *113*, 192–200.
- (28) Waisbren, B. A.; Spink, W. W. *Ann. Intern. Med.* **1950**, *33*, 1099–1119.
- (29) Jin, Y.; Jang, J. W.; Lee, M. H.; Han, C. H. *Clin. Chim. Acta* **2006**, *364*, 260–266.

**Scheme 3.** Hydrolysis of PPE<sub>y</sub> To Produce Anionic-PPE<sub>y</sub>

than those in the purposely doped PPEs. We proposed that these inherent anthryl defects were responsible for the polymer's highly emissive, excimer-like fluorescence<sup>30</sup> in aggregated solutions and films. These polymers were originally designed with electron-withdrawing perfluoroalkyl side chains and ester groups to develop high ionization potential conjugated polymers for detecting electron-rich aromatic compounds.<sup>31</sup>

For the present study, we first investigated the aggregation behavior of two polymers, PPE<sub>0</sub> and PPE<sub>2</sub>, and their respective polyanionic, carboxylate derivatives, anionic-PPE<sub>0</sub> and anionic-PPE<sub>2</sub>, which were synthesized using a post-polymerization hydrolysis reaction<sup>32</sup> (Scheme 3).

The hydrolysis reaction to produce anionic-PPE<sub>y</sub> involved heating a solution of PPE<sub>y</sub> ( $M_n = 19$  kDa for PPE<sub>0</sub>; 23 kDa for PPE<sub>2</sub>) in a tetrahydrofuran/water cosolvent mixture containing 0.10 M lithium hydroxide at 40 °C for 2 days. The hydrolyzed polymer was purified by dialysis against distilled water, using regenerated cellulose dialysis tubing with a molecular weight cutoff of 10 kDa. The carboxylate-containing anionic-PPE<sub>y</sub> was then characterized by <sup>1</sup>H NMR and attenuated total reflection infrared (ATR-IR) spectroscopy, and their spectra were compared with those of their parent polymers, PPE<sub>y</sub>. The <sup>1</sup>H NMR spectra of anionic-PPE<sub>y</sub> showed no remaining methyl ester signals around 3.9 ppm, consistent with a complete hydrolysis reaction. ATR-IR spectra revealed a shift of the carbonyl stretching band from 1723 cm<sup>-1</sup> in the parent polymers to 1710 cm<sup>-1</sup> in the hydrolyzed polymers, accompanied by a new, broad hydroxyl stretching band around 3421 cm<sup>-1</sup>. The ATR-IR data is consistent with the conversion of ester groups to carboxylate/carboxylic acid groups.

**Solvent-Induced Aggregation.** The aggregation behavior of both sets of PPE<sub>y</sub> and anionic-PPE<sub>y</sub> was studied in cosolvent mixtures of “good solvent” and “poor solvent”. With respect to a specific polymer, a good solvent is one in which the polymer is in an expanded and well-dissolved state, and a poor solvent is one in which the polymer is in a collapsed or aggregated state.<sup>33</sup> Before hydrolysis, the parent polymers, PPE<sub>y</sub>, were insoluble in polar protic solvents such as water, methanol, and

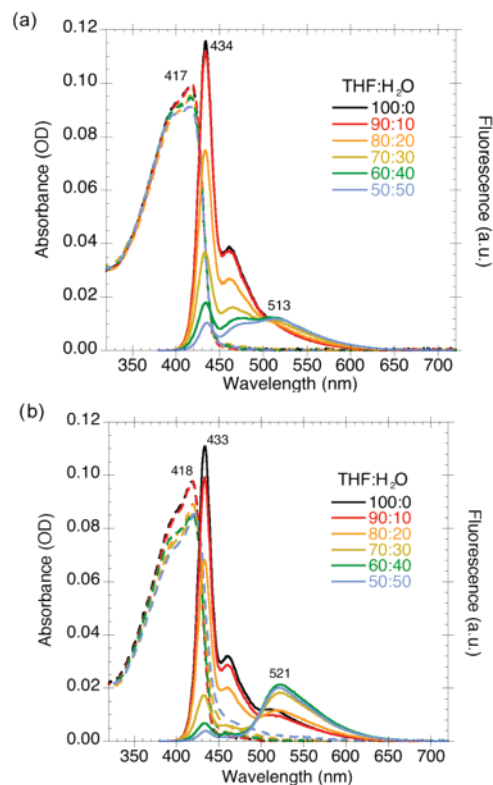


**Figure 1.** Absorption (dashed) and fluorescence (solid) spectra of (a) PPE<sub>0</sub><sup>16</sup> and (b) PPE<sub>2</sub> in solutions of tetrahydrofuran/water (v:v).

ethanol.<sup>34</sup> However, after hydrolysis, the resulting polymers, anionic-PPE<sub>y</sub>, were very soluble in methanol and ethanol and partially soluble in water. Expectedly, less polar, aprotic solvents such as chloroform and tetrahydrofuran effectively dissolved PPE<sub>y</sub>, but not anionic-PPE<sub>y</sub>. To investigate the aggregation behavior of the polymers, we chose the good solvent/poor solvent mixtures of tetrahydrofuran/water for PPE<sub>y</sub> (Figure 1) and ethanol/hexane for anionic-PPE<sub>y</sub> (Figure 2). The polymers were aggregated in various good solvent/poor solvent ratios and studied by UV-vis absorption and fluorescence spectroscopy.

For both sets of PPE<sub>y</sub> and anionic-PPE<sub>y</sub>, the solutions in 100% good solvent appeared fluorescent blue, as characterized by the sharp emission band around 430–434 nm and the absence of any green emission bands around 500–521 nm. Upon addition of the corresponding poor solvent, the polymers began to aggregate. As explained earlier, aggregation of conjugated polymers is usually accompanied by self-quenching as well as enhanced exciton transport properties. Since the anthryl-doped polymers, PPE<sub>2</sub> and anionic-PPE<sub>2</sub>, contained significant quantities of low-energy anthryl units, their photogenerated excitons were efficiently funneled to these exciton traps under aggregation conditions (low good solvent/poor solvent ratios). The excited anthryl units could then emit their low-energy green light (500–521 nm), which became increasingly significant as the degree of aggregation increased. As expected, the polymers containing the additional anthryl units, PPE<sub>2</sub> and anionic-PPE<sub>2</sub>, exhibited greater enhancements of the green emission bands upon aggregation than the undoped polymers, PPE<sub>0</sub> and anionic-PPE<sub>0</sub> (Table 2).

(30) Kim, Y.; Bouffard, J.; Kooi, S. E.; Swager, T. M. *J. Am. Chem. Soc.* **2005**, *127*, 13726–13731.

(31) Kim, Y.; Whitten, J. E.; Swager, T. M. *J. Am. Chem. Soc.* **2005**, *127*, 12122–12130.

(32) Kim, Y. M.; Swager, T. M. *Macromolecules* **2006**, *39*, 5177–5179.

(33) Flory, P. J. *Principles of Polymer Chemistry*; Cornell University Press: Ithaca, NY, 1953.

(34) The dielectric constant of the solvents used in this study are hexane, 1.89; chloroform, 4.81; tetrahydrofuran, 7.52; ethanol, 25.3; methanol, 33.0; water, 78. These values were taken from Lide, D. R. *Handbook of Organic Solvents*; CRC Press: Boca Raton, FL, 1995 and Atkins, P. W. *Physical Chemistry*, 6th ed.; Freeman: New York, 1998.

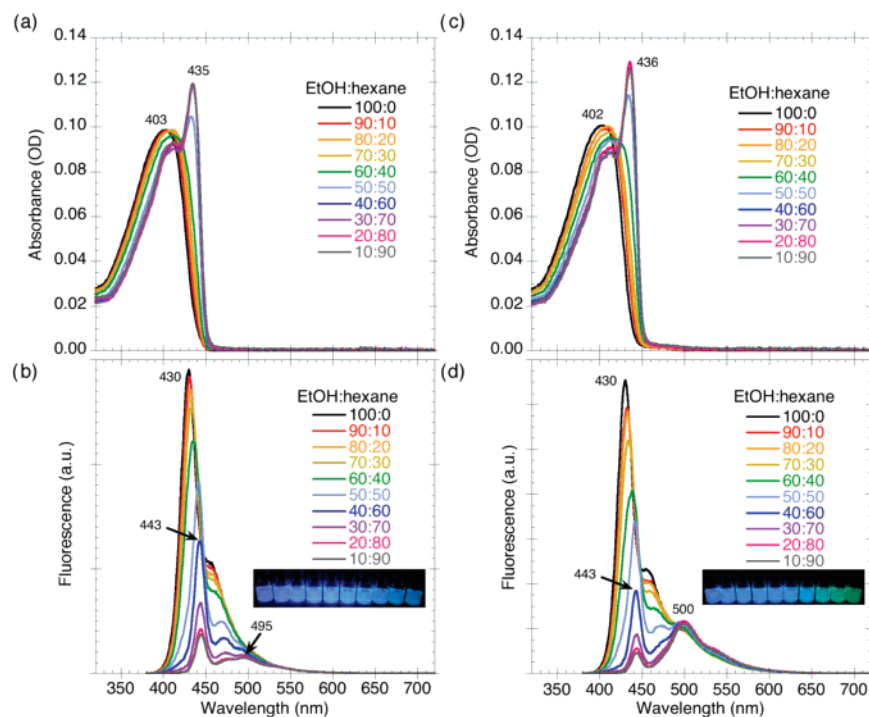


**Figure 2.** Absorption (top) and fluorescence (bottom) spectra of anionic-PPE<sub>0</sub> (left) and anionic-PPE<sub>2</sub> (right) in solutions of ethanol/hexane (v:v). Insets: fluorescence photographs of the corresponding solutions in order of increasing aggregation from left to right, irradiated with a 365-nm mercury lamp.

**Table 2.** Ratios of the Green Band Maximum Fluorescence Intensity to the Blue Band Maximum Fluorescence Intensity ( $I_{\text{green}}/I_{\text{blue}}$ ) in Aggregated Polymer Solutions<sup>a</sup>

aggregated polymer solution	$I_{\text{green}}/I_{\text{blue}}$
PPE <sub>0</sub> in 50:50 THF/H <sub>2</sub> O	1.15
PPE <sub>2</sub> in 50:50 THF/H <sub>2</sub> O	4.98
anionic-PPE <sub>0</sub> in 10:90 EtOH/hexane	0.402
anionic-PPE <sub>2</sub> in 10:90 EtOH/hexane	2.39

<sup>a</sup> The  $I_{\text{green}}/I_{\text{blue}}$  ratios were calculated from the fluorescence intensities at the following blue and green wavelengths, respectively: PPE<sub>0</sub>, 435 nm, 513 nm; PPE<sub>2</sub>, 434 nm, 521 nm; anionic-PPE<sub>0</sub>, 445 nm, 495 nm; anionic-PPE<sub>2</sub>, 444 nm, 500 nm.

Upon aggregation in  $\leq 50:50$  ethanol/hexane cosolvent mixtures, the previously colorless anionic-PPE<sub>y</sub> solutions exhibited new absorption bands around 435–436 nm, resulting in slightly yellow solutions. However, the transition from colorless to slightly yellow was not very noticeable to the naked eye. The new, red-shifted absorption band was attributed to the increase of the effective conjugation length of the PPE due to aggregation-induced planarization of the polymer chains.<sup>35–37</sup> This planarization can also explain the slight shift of the blue emission band at 430 nm to longer wavelengths (around 443 nm).

The solvent-induced aggregation in all four PPE solutions was accompanied by enhanced exciton migration; however, only the PPEs containing appreciable amounts of green-emitting exciton traps (i.e., the low-energy anthryl units) exhibited a visually noticeable fluorescence color change upon aggregation.

**Aggregation-Based Sensing of Nonquenching Multicationic Analytes.** Since anionic-PPE<sub>2</sub> displayed a visually noticeable blue-to-green fluorescence color change upon aggregation in poor solvents, we investigated the fluorescence

response of this polymer to oppositely charged, small-molecule analytes. More specifically, we were interested in detecting polyamines (e.g., spermine and spermidine) and aminoglycosides (e.g., neomycin), which are biologically relevant, multicationic analytes that cannot directly quench the polymer fluorescence by electron transfer or energy transfer mechanisms.

We first studied the analyte-induced aggregation of the polymer in ethanol. Figure 3 shows the absorption, fluorescence, and normalized fluorescence spectra of anionic-PPE<sub>2</sub> upon addition of spermine. As the concentration of spermine increased, the absorption spectra exhibited a new band around 430 nm, and the inherent blue emission band of the PPE shifted to longer wavelengths, consistent with the aggregation-induced planarization of the polymer chains.<sup>35</sup> The normalized fluorescence spectra clearly display the aggregation-induced enhancement of the green emission band (510 nm) relative to the blue emission band (430–445 nm) as the spermine concentration increased. Evidently, the multicationic, small-molecule analyte was able to effectively induce aggregation between the PPE chains and generate a blue-to-green fluorescence color change.

Since biologically relevant analytes, such as polyamines and aminoglycosides, are naturally found in aqueous fluids, we wanted to use a more practical solvent system in which to test the chemical sensor. Unfortunately, anionic-PPE<sub>2</sub> was only partially soluble in water due to the hydrophobic nature of its polymer backbone, aromatic moieties, and perfluorinated alkyl side chains. However, in an ethanol/water cosolvent system, the polymer can be well dissolved. Figure 4 shows the absorption and fluorescence spectra of anionic-PPE<sub>2</sub> in various ethanol/water cosolvent ratios (without any analytes). The absorption spectra (Figure 4a) show that the 50:50 EtOH/H<sub>2</sub>O solution had a small absorption shoulder around 435 nm, indicating the onset of the planarization and aggregation of the PPE chains.

(35) Miteva, T.; Palmer, L.; Kloppenburg, L.; Neher, D.; Bunz, U. H. F. *Macromolecules* **2000**, *33*, 652–654.

(36) Rughoopath, S. D. D. V.; Hotta, S.; Heeger, A. J.; Wudl, F. *J. Polym. Sci., Part B: Polym. Phys.* **1987**, *25*, 1071–1078.

(37) Leclerc, M. *Adv. Mater.* **1999**, *11*, 1491–1498.

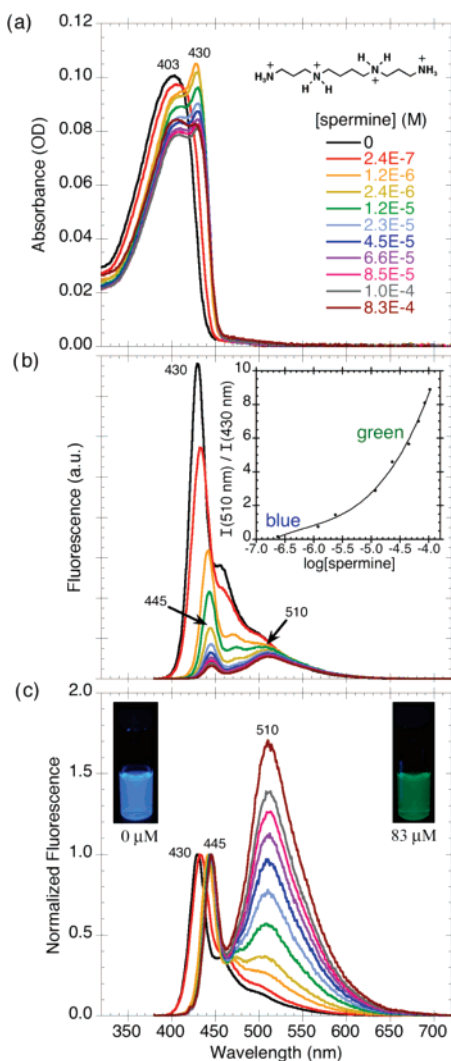


**Figure 3.** (a) Absorption and (b) fluorescence spectra of anionic-PPE<sub>2</sub> in ethanol, upon addition of spermine. (c) Fluorescence spectra normalized to the blue emission (430–445 nm) intensity maximum. Insets: structure of fully protonated spermine; graph of the ratio of fluorescence intensity at 510 nm to that at 430 nm, as a function of the logarithm of spermine concentration; fluorescence photographs of the 0 and 83  $\mu\text{M}$  solutions.

Since the polymer was on the threshold of aggregation at this solvent ratio, the addition of oppositely charged analytes to this solution might lead to aggregation at even lower concentrations than in ethanol. Figure 5 shows that, indeed, anionic-PPE<sub>2</sub> in a 50:50 EtOH/H<sub>2</sub>O solution containing a low concentration (0.69  $\mu\text{M}$ ) of spermine formed aggregated polymer chains that exhibited enhanced green emission. In comparison, the polymer in ethanol solution (Figure 3) experienced a more gradual fluorescence color change upon addition of spermine and required  $>23 \mu\text{M}$  of the polyamine to appear fluorescent green. Therefore, a more sensitive response was achieved by using a starting solution that was already partially aggregated. The fluorescence photographs in Figure 5c show that a visually noticeable blue-to-green fluorescence color change occurred upon aggregation of the PPE chains.

The PPE aggregation was promoted by complexation between the polyanionic PPE and the multicationic, small-molecule analyte. Spermine, which has  $pK_a$  values of 11.50, 10.95, 9.79,

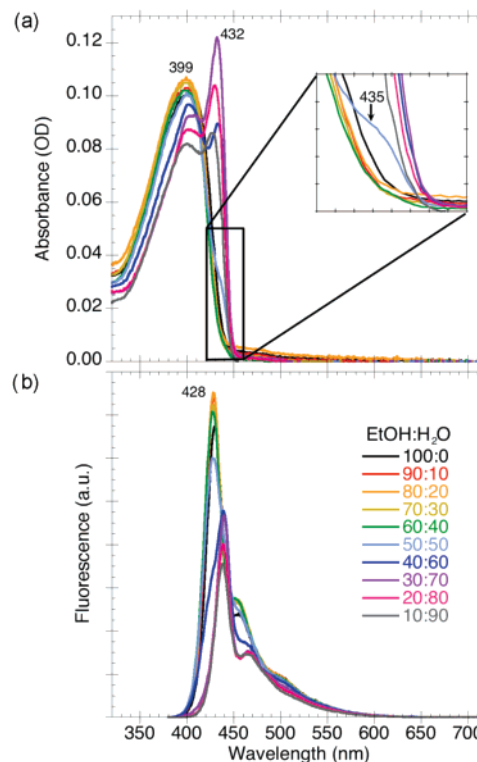


**Figure 4.** (a) Absorption and (b) fluorescence spectra of anionic-PPE<sub>2</sub> in solutions of ethanol/water (v:v). Inset: enlarged region of the absorption spectrum showing the onset of the aggregation-induced absorption band around 435 nm.

and 8.90,<sup>38</sup> should predominantly have a +4 charge in the 50:50 EtOH/H<sub>2</sub>O solution (pH = 5.5 throughout the experiment). The multiple charged sites in spermine effectively attracted and bound multiple PPE chains, resulting in many interchain contacts between the polymer chains. The aggregated PPE chains, with their enhanced exciton transport properties, exhibited efficient exciton trapping by the emissive, low-energy anthryl sites, resulting in the enhanced green emission (Figure 6).

In a buffered 50:50 EtOH/H<sub>2</sub>O solution (20 mM sodium acetate/acetic acid, pH 6.0), anionic-PPE<sub>2</sub> exhibited a less sensitive response to the addition of spermine (Figure 7) due to the charge screening effects of the buffer ions.<sup>39,40</sup> Additionally, the higher ionic strength of the solution enhanced the hydrophobic interactions between the polymers, resulting in preaggregation,<sup>8,17,41</sup> which was accompanied by a red-shift of the blue fluorescence band (from 429 to 439 nm). However, the short-wavelength shoulder of the blue fluorescence band suggested that not all PPE chains underwent aggregation-induced planarization. The charge-screening effects of the buffer ions may have stabilized some polymer chains in an isolated, random coil conformation. However, upon addition of spermine, a noticeable fluorescence color change was still observed, albeit with less color contrast (from blue to bluish green, Figure 7b inset) than that observed for the solution without the buffer ions.

To probe the selectivity of the CPE sensor, we investigated its optical response to two other naturally occurring polyamines,

- (38) Takeda, Y.; Samejima, K.; Nagano, K.; Watanabe, M.; Sugeta, H.; Kyogoku, Y. *Eur. J. Biochem.* **1983**, *130*, 383–389.  
 (39) Wang, J.; Wang, D. L.; Miller, E. K.; Moses, D.; Bazan, G. C.; Heeger, A. J. *Macromolecules* **2000**, *33*, 5153–5158.  
 (40) Kim, I. B.; Dunkhorst, A.; Gilbert, J.; Bunz, U. H. F. *Macromolecules* **2005**, *38*, 4560–4562.  
 (41) Wosnick, J. H.; Mello, C. M.; Swager, T. M. *J. Am. Chem. Soc.* **2005**, *127*, 3400–3405.

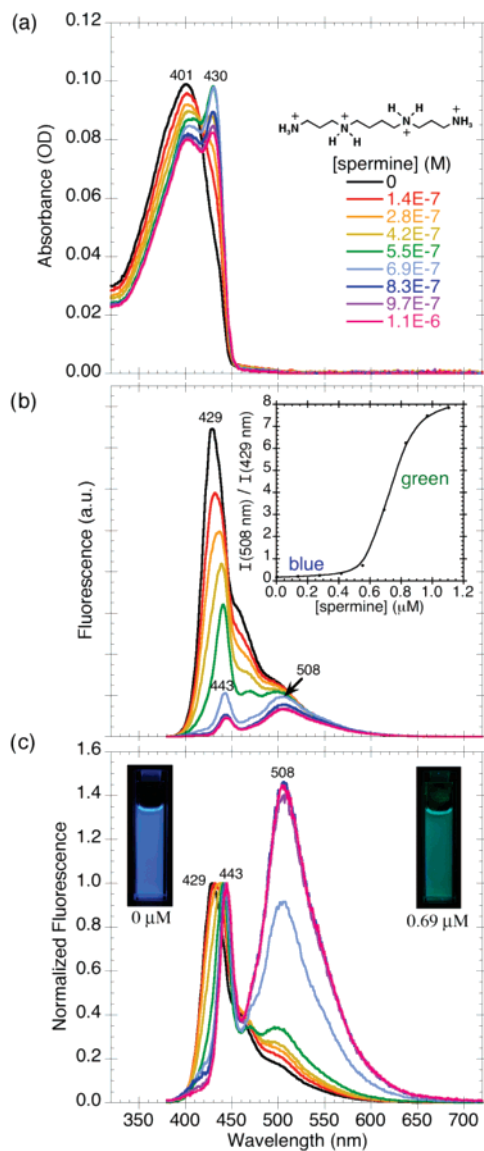


**Figure 5.** (a) Absorption, (b) fluorescence, and (c) normalized fluorescence spectra of anionic-PPE<sub>2</sub> in 50:50 EtOH/H<sub>2</sub>O, upon addition of spermine. Insets: structure of fully protonated spermine; graph of the ratio of fluorescence intensity at 508 nm to that at 429 nm, as a function of spermine concentration; fluorescence photographs of the 0 and 0.69  $\mu$ M solutions.

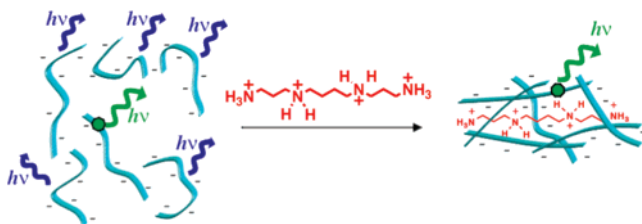


**Figure 6.** Schematic illustration of the spermine-induced aggregation of the anionic conjugated polyelectrolyte and the accompanying blue-to-green fluorescence color change.

spermidine and putrescine, and also to a monocationic amine, *n*-butylamine (Figure 8).

Similar to the response toward spermine, the polyanionic polymer also formed complexes with spermidine ( $pK_a = 11.56, 10.80, 9.52$ ),<sup>38</sup> which should predominantly have a +3 charge in the 50:50 EtOH/H<sub>2</sub>O solution (pH = 5.5 throughout the experiment). The analyte-induced aggregation of the PPE chains

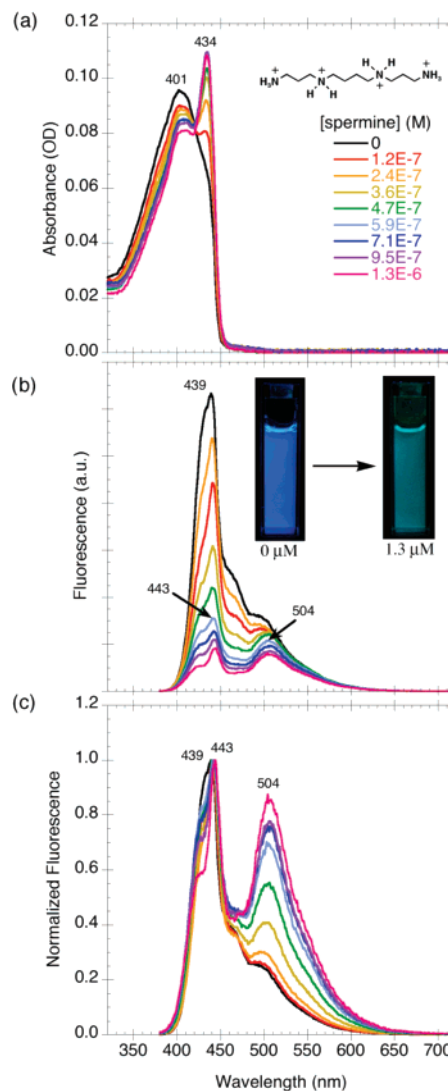


**Figure 7.** (a) Absorption, (b) fluorescence, and (c) normalized fluorescence spectra of anionic-PPE<sub>2</sub> in a buffered 50:50 EtOH/H<sub>2</sub>O solution (20 mM NaOAc/COOH, pH 6.0), upon addition of spermine. Insets: structure of fully protonated spermine; fluorescence photographs of the 0 and 1.3  $\mu$ M solutions.

was accompanied by a blue-to-green fluorescence color change (Figure 8a–c). The 50:50 EtOH/H<sub>2</sub>O solution of anionic-PPE<sub>2</sub> required 1.6  $\mu$ M spermidine to become fluorescent green. In comparison, it needed only 0.69  $\mu$ M spermine to achieve a similar visual response (Figure 5). Therefore, the anionic-PPE<sub>2</sub> solution was more sensitive toward the detection of spermine (+4 charged) than spermidine (+3 charged). This sensitivity can be explained by the better ability of spermine at aggregating the polyanionic PPE chains since it had an additional positively charged site to electrostatically attract and bind negatively charged polymer chains, thus leading to denser polymer aggregates. The number of charges on an analyte has been previously demonstrated to be an important factor in the optical responses of other conjugated polyelectrolyte sensors.<sup>6,42–45</sup> The

(42) Wang, D. L.; Wang, J.; Moses, D.; Bazan, G. C.; Heeger, A. J.; Park, J. H.; Park, Y. W. *Synth. Met.* **2001**, *119*, 587–588.

(43) Wang, D. L.; Wang, J.; Moses, D.; Bazan, G. C.; Heeger, A. J. *Langmuir* **2001**, *17*, 1262–1266.

(44) Tan, C. Y.; Alas, E.; Muller, J. G.; Pinto, M. R.; Kleiman, V. D.; Schanze, K. S. *J. Am. Chem. Soc.* **2004**, *126*, 13685–13694.

(45) Li, C.; Numata, M.; Takeuchi, M.; Shinkai, S. *Angew. Chem., Int. Ed.* **2005**, *44*, 6371–6374.

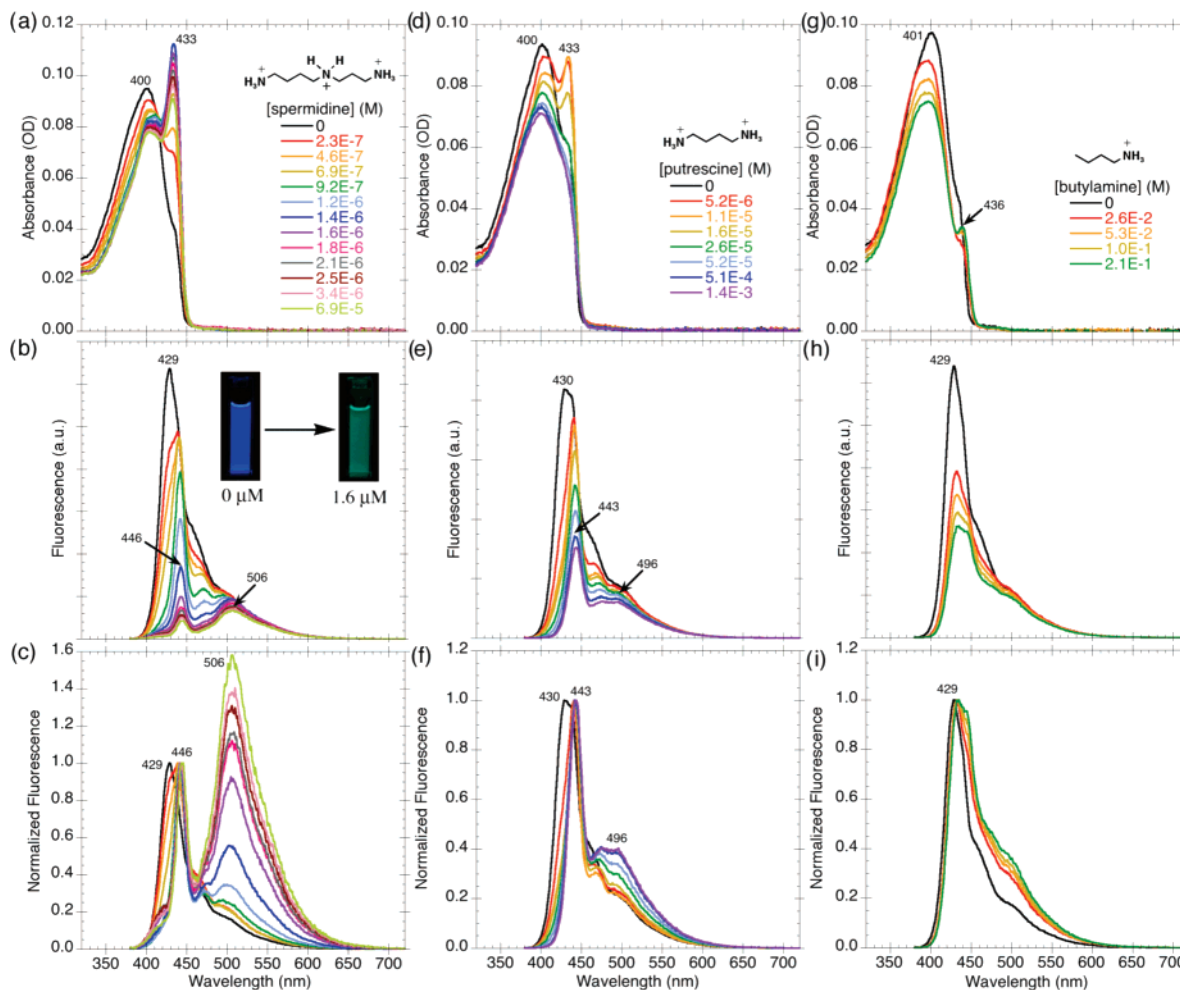


**Figure 8.** Absorption (top row), fluorescence (middle row), and normalized fluorescence (bottom row) spectra of anionic-PPE<sub>2</sub> in 50:50 EtOH/H<sub>2</sub>O (without buffer), upon addition of spermidine (left column), putrescine (middle column), and *n*-butylamine (right column). Insets: structures of fully protonated spermidine, putrescine, and *n*-butylamine; fluorescence photographs of the 0 and 1.6  $\mu\text{M}$  spermidine solutions.

threshold concentrations of spermine (0.69  $\mu\text{M}$ ) and spermidine (1.6  $\mu\text{M}$ ) to induce a fluorescence color change in anionic-PPE<sub>2</sub> may be low enough to develop an assay (in aqueous/ethanol solutions) for detecting the urinary concentration differences between cancer patients and healthy volunteers (Table 1).

Expectedly, anionic-PPE<sub>2</sub> demonstrated poor sensitivities toward putrescine ( $\text{p}K_{\text{a}} = 10.65, 9.20$ ; +2 charged)<sup>46</sup> and *n*-butylamine ( $\text{p}K_{\text{a}} = 10.64$ ; +1 charged).<sup>46</sup> Neither putrescine nor *n*-butylamine induced a visible blue-to-green fluorescence color change in the PPE solutions, even at relatively high concentrations (Figure 8d–i). However, both analytes were able to promote planarization and a small degree of aggregation (possibly dimerization) between the polymer chains, as evidenced by the red-shifted absorption band (around 433–436 nm) and fluorescence self-quenching. Similarly, Lavigne et al. recently reported an aggregation-based CPE sensor that exhibited different absorption spectra in the presence of structurally similar amines.<sup>47–49</sup> In our fluorescent sensory scheme, putrescine and *n*-butylamine were significantly less effective than spermine and

spermidine at binding multiple PPE chains to form tightly associated aggregates with enhanced interchain exciton migration. Therefore, a chemical sensor based on nonspecific electrostatic interactions may still exhibit some selectivity between similar analytes.<sup>40,45,47,50</sup>

We next investigated another biologically relevant analyte, neomycin (Scheme 2), which is an aminoglycoside antibiotic containing six primary amine groups ( $\text{p}K_{\text{a}} = 8.80, 8.60, 8.04, 7.60, 7.55, \text{ and } 5.74$ )<sup>51</sup> and is, therefore, expected to induce a similar sensor response as the polyamines. In a 50:50 ethanol/water solution ( $\text{pH} = 5.5$  throughout the experiment), this multicationic, small-molecule analyte effectively induced aggregation between the anionic-PPE<sub>2</sub> chains, resulting in a visually noticeable blue-to-green fluorescence color change at a concentration of 0.92  $\mu\text{M}$ , or 570  $\mu\text{g/L}$  (Figure 9). This low detection level, in addition to the very rapid response, makes this sensor potentially suitable for monitoring neomycin residue levels in milk,<sup>29,52</sup> which currently has a maximum residue limit of 1500  $\mu\text{g/kg}$  ( $\sim 1500 \mu\text{g/L}$ ), as established by the European Union.<sup>20</sup>

Since this CPE-based sensor relies on nonspecific electrostatic interactions, it will inherently be susceptible to interference from

(46) Martell, A. E.; Smith, R. M. *Critical Stability Constants*; Plenum Press: New York, 1974; Vol. 2.

(47) Nelson, T. L.; O'Sullivan, C.; Greene, N. T.; Maynor, M. S.; Lavigne, J. *J. Am. Chem. Soc.* **2006**, *128*, 5640–5641.

(48) Maynor, M. S.; Nelson, T. L.; O'Sullivan, C.; Lavigne, J. *J. Org. Lett.* **2007**, *9*, 3217–3220.

(49) Nelson, T. L.; Tran, I.; Ingallinera, T. G.; Maynor, M. S.; Lavigne, J. *J. Analyst* **2007**, *132*, 1010–1023.

(50) Sandanaraj, B. S.; Demont, R.; Aathimankandan, S. V.; Savariar, E. N.; Thayumanavan, S. *J. Am. Chem. Soc.* **2006**, *128*, 10686–10687.

(51) Botto, R. E.; Coxon, B. *J. Am. Chem. Soc.* **1983**, *105*, 1021–1028.

(52) Shaikh, B.; Jackson, J. *J. Liq. Chromatogr.* **1989**, *12*, 1497–1515.

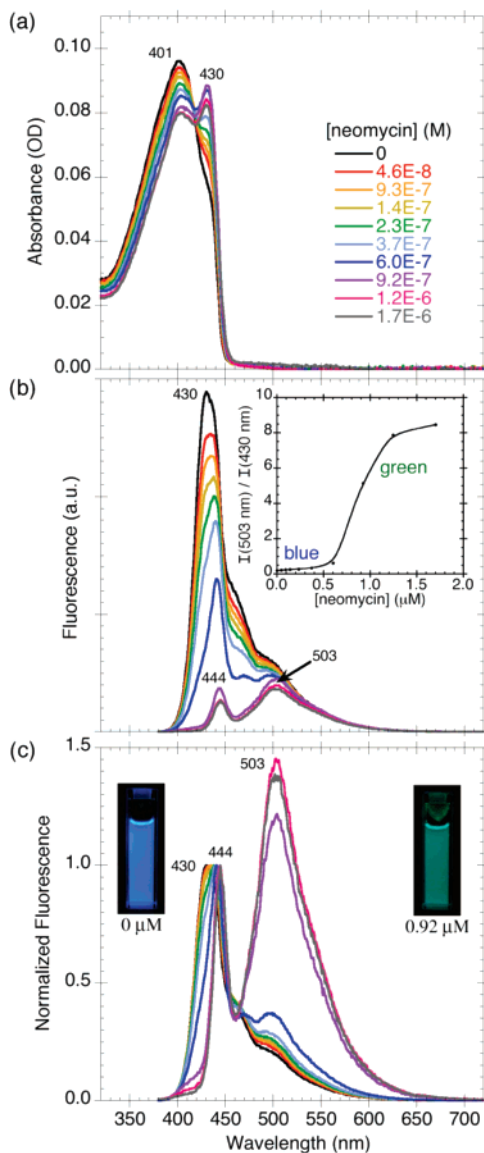


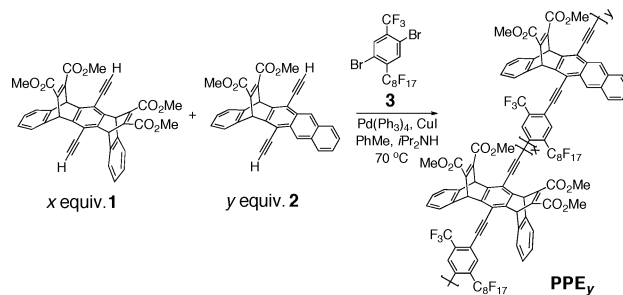
**Figure 9.** (a) Absorption, (b) fluorescence, and (c) normalized fluorescence spectra of anionic-PPE<sub>2</sub> in 50:50 EtOH/H<sub>2</sub>O, upon addition of neomycin. Insets: graph of the ratio of fluorescence intensity at 503 nm to that at 430 nm, as a function of neomycin concentration; fluorescence photographs of the 0 and 0.92  $\mu\text{M}$  solutions.

multiply charged species, such as proteins and multivalent cations, commonly found in complex biological fluids.<sup>15,53</sup> Therefore, removal of these interfering species from biological samples would be necessary before analysis using nonspecific polyelectrolyte sensors<sup>3</sup> such as anionic-PPE<sub>2</sub>.

## Conclusions

In summary, an anthryl-doped, polyanionic poly(*p*-phenylene ethynylene) was synthesized and spectroscopically characterized under various aggregation conditions. In dilute solution, this polyanionic polymer formed tightly associated aggregates upon addition of a poor solvent or upon addition of nonquenching, multicationic, small-molecule analytes (spermine, spermidine, and neomycin). The induced aggregation of the conjugated polymer chains resulted in enhanced exciton migration from

## Scheme 4. Synthesis of PPE<sub>y</sub>



the blue-emitting PPE segments to the green-emitting anthryl units. The rapid, visually noticeable, blue-to-green fluorescence color change that accompanies aggregation of this polymer may be useful in sensor arrays for detecting biologically relevant, nonquenching, multicationic species.

## Experimental Section

**General Methods and Instrumentation.** Synthetic manipulations were carried out under an argon atmosphere using standard Schlenk techniques. <sup>1</sup>H NMR spectra were recorded on a Varian 500 MHz spectrometer. Chemical shifts of each signal were reported in units of  $\delta$  (ppm) and referenced to the residual proton signal of the solvent (chloroform-*d*: 7.27; methanol-*d*: 3.31). Splitting patterns were designated as s (singlet), d (doublet), t (triplet), q (quartet), m (multiplet), and br (broad). ATR-IR spectra were obtained on a NEXUS 870 spectrometer.

Polymer molecular weights were determined by gel permeation chromatography (GPC) versus polystyrene standards (Agilent Technologies, Inc.) using THF as the eluent at a flow rate of 1.0 mL/min in a Hewlett-Packard series 1100 GPC system equipped with three PLgel 5  $\mu\text{m}$  10<sup>5</sup>, 10<sup>4</sup>, 10<sup>3</sup> (300  $\times$  7.5 mm) columns in series and a diode array detector at 254 nm.

The UV-vis absorption and fluorescence spectra were measured in a 1-cm quartz cuvette at a repeating unit concentration of about  $2.7 \times 10^{-6}$  M with an optical density of 0.09–0.10 at the  $\lambda_{\text{max}}$  around 399–418 nm. UV-vis absorption spectra were measured with a Cary 50 UV-vis absorption spectrometer at room temperature. Fluorescence spectra were measured with a SPEX Fluorolog- $\tau$ 2 fluorometer (model FL112, 450 W xenon lamp). Fluorescence spectra were obtained at a right-angle geometry using an excitation wavelength of 375 nm.

Aggregate solutions in good solvent/poor solvent mixtures were prepared by dropwise addition of the poor solvent into a stirring solution of the polymer dissolved in a good solvent. Analyte-induced aggregation experiments were performed by the sequential addition of a measured volume of stock solution directly into the cuvette for absorption and fluorescence measurements. Each stock solution contained a concentrated amount of the target analyte, and it also contained the same concentration of anionic-PPE<sub>2</sub> as the solution without any analyte. The pH of the solutions were measured by colorpHast pH-indicator strips (EMD) or by a  $\phi$  350 pH meter (Beckman Instruments, Inc.).

**Materials.** All solvents were of spectral grade unless otherwise noted. Water for spectroscopic measurements was obtained from a Millipore Milli-Q purification system. Pd(PPh<sub>3</sub>)<sub>4</sub> was purchased from Strem Chemicals, Inc. Spermine and spermidine were purchased from Alfa Aesar. Aqueous neomycin solution (1 mg/mL) was purchased from Fluka. The synthesis and characterization of PPE<sub>0</sub> was reported elsewhere.<sup>16</sup> All other chemicals were purchased from Aldrich Chemical Co., Inc., and used as received.

**Synthetic Procedures. PPE<sub>2</sub>.** The doped polymer was synthesized according to ref 16 (Scheme 4) as follows: To a 25-mL Schlenk tube were added **1** (90.8 mg,  $1.49 \times 10^{-4}$  mol), **2** (162  $\mu\text{L}$  of a 17.9 mM CHCl<sub>3</sub> solution,  $2.92 \times 10^{-6}$  mol), and **3** (104.7 mg,  $1.45 \times 10^{-4}$  mol). The solvent was evaporated at 33  $^{\circ}\text{C}$  under a flow of nitrogen, and

(53) Kim, I. B.; Dunkhorst, A.; Bunz, U. H. F. *Langmuir* **2005**, *21*, 7985–7989.



then the mixture was dried in vacuo. Under a nitrogen atmosphere, Pd(PPh<sub>3</sub>)<sub>4</sub> (16.8 mg, 1.5 × 10<sup>-5</sup> mol) and CuI (16.6 mg, 8.7 × 10<sup>-5</sup> mol) were added. The vessel was evacuated and back-filled with argon three times, followed by the addition of degassed 7:3 toluene/diisopropylamine (4.0 mL). The mixture was stirred at 70 °C for 3 days under an argon atmosphere. The mixture was then subjected to a workup with CHCl<sub>3</sub> and a saturated aqueous NH<sub>4</sub>Cl solution. The organic phase was washed with water, then brine. The organic extract was dried over MgSO<sub>4</sub> and filtered before solvent removal under reduced pressure. The residue was dissolved in CHCl<sub>3</sub> and then added dropwise in rapidly stirring methanol. The mixture was centrifuged at 3000 rpm for 30 min and then decanted. The polymer was then washed with additional MeOH, and the mixture was centrifuged and decanted again. The solid polymer was then dissolved in acetone, transferred to a vial, then dried in vacuo to afford a yellow solid (158.8 mg, ~94%). *M<sub>n</sub>* = 23 kDa, PDI = 3.24. <sup>1</sup>H NMR (500 MHz, CDCl<sub>3</sub>): 8.50–8.44 (1H, br), 8.28–8.22 (1H, br), 8.12 (0.15H, s), 8.01 (0.10H, d, *J* = 8.3 Hz), 7.82 (0.06H, d, *J* = 8.3 Hz), 7.72–7.54 (0.46H, br), 7.50–7.36 (4H, br), 7.15–6.98 (4H, br), 6.10–5.96 (4H, br), 3.93–3.83 (12H, br). ATR–IR (ν/cm<sup>-1</sup>): 2956, 2852, 1722, 1641, 1514, 1437, 1209, 1142, 1061, 818, 748, 677.

**Anionic-PPE<sub>0</sub> and Anionic-PPE<sub>2</sub>.** These polymers were prepared similarly, and a general procedure is illustrated by the following synthesis of anionic-PPE<sub>0</sub>. To a 25-mL Schlenk tube were added a 4.5-mL solution of PPE<sub>0</sub><sup>16</sup> (*M<sub>n</sub>* = 19 kDa, 28 mg, 0.023 mmol repeat units) dissolved in degassed THF, then a 2.0 mL solution of 0.30 M

LiOH in degassed water. After stirring the mixture at 40 °C for 2 days, we removed the solvent in vacuo. The hydrolyzed polymer was then subjected to dialysis against pure water for 3 days, using SnakeSkin dialysis tubing (Pierce) with a molecular weight cutoff of 10 kDa. The water was removed in vacuo to afford anionic-PPE<sub>0</sub> as a dark yellow solid (27 mg, 100%). <sup>1</sup>H NMR (500 MHz, CD<sub>3</sub>OD): 8.80–8.72 (1H, br), 8.60–8.53 (1H, br), 8.25 (0.19H, s), 8.16 (0.10H, d, *J* = 8.5 Hz), 7.97 (0.12H, d, *J* = 8.5 Hz), 7.77–7.62 (0.40H, br), 7.51–7.39 (4H, br), 7.15–6.98 (4H, br), 6.55–6.38 (4H, br). ATR–IR (ν/cm<sup>-1</sup>): 3421, 2929, 2856, 1711, 1587, 1512, 1469, 1408, 1373, 1306, 1209, 1146, 750, 677, 634, 598.

**Anionic-PPE<sub>2</sub>.** Reagents: 16-mL solution of PPE<sub>2</sub> (*M<sub>n</sub>* = 23 kDa, 100 mg, ~0.085 mmol repeat units) dissolved in THF, 4.0-mL aqueous solution of 0.53 M LiOH. Yield: 91 mg (96%). <sup>1</sup>H NMR (500 MHz, CD<sub>3</sub>OD): 8.80–8.70 (1H, br), 8.62–8.51 (1H, br), 8.41 (0.15H, br), 8.10–8.06 (0.06H, br), 7.95–7.85 (0.13H, br), 7.68–7.58 (0.27H, br), 7.53–7.33 (4H, br), 7.12–6.90 (4H, br), 6.65–6.35 (4H, br). ATR–IR (ν/cm<sup>-1</sup>): 3421, 2925, 2856, 1709, 1583, 1510, 1471, 1404, 1371, 1304, 1209, 1144, 750, 677, 633, 598.

**Acknowledgment.** This work was supported by the U.S. Army through the Institute for Soldier Nanotechnologies, under Contract DAAD-19-02-0002 with the U.S. Army Research Office and NIH Grant 1-U01-HL080731 (Project 4).

JA075573R